RSC Advances

This is an *Accepted Manuscript*, which has been through the Royal Society of Chemistry peer review process and has been accepted for publication.

Accepted Manuscripts are published online shortly after acceptance, before technical editing, formatting and proof reading. Using this free service, authors can make their results available to the community, in citable form, before we publish the edited article. This *Accepted Manuscript* will be replaced by the edited, formatted and paginated article as soon as this is available.

You can find more information about *Accepted Manuscripts* in the Information for Authors.

Please note that technical editing may introduce minor changes to the text and/or graphics, which may alter content. The journal's standard Terms & Conditions and the Ethical guidelines still apply. In no event shall the Royal Society of Chemistry be held responsible for any errors or omissions in this *Accepted Manuscript* or any consequences arising from the use of any information it contains.

ROYAL SOCIETY OF CHEMISTRY

www.rsc.org/advances

Biocompatibility Evaluation of Novel β-Type Titanium Alloy $(Ti\text{-}35Nb\text{-}7Zr\text{-}5Ta)_{98}Si_2$ *In Vitro*

Yu Sun,[a] Yang Song,[b] Jianlin Zuo,[c] Shengqun Wang[d] and Zhongli Gao*[a]

RSC Advances Accepted Manuscript

Abstract

Background: Low elastic modulus and high strength are two critical requirements for orthopedic implant materials. A newly reported ultrafine-grained β-type titanium alloy $(Ti\text{-}35Nb\text{-}7Zr\text{-}5Ta)_{98}Si_2$, which was designed by d-electron alloy design theory and fabricated by spark plasma sintering, exhibits both low elastic modulus and high strength. However, its biocompatibility remains largely unclear.

Methods: The microstructure of the $(Ti\text{-}35Nb\text{-}7Zr\text{-}5Ta)_{98}Si_2$ alloy was examined by scanning electron microscopy. Its effects on fibroblast cell proliferation and osteoblast cell adhesion, morphology, differentiation, inflammatory response, apoptosis, and biomineralization were investigated in *in vitro* studies. The commercial Ti6Al4V alloy was studied side-by-side for comparison.

Results: The $(Ti\text{-}35Nb\text{-}7Zr\text{-}5Ta)_{98}Si_2$ alloy displayed a two-phase microstructure, in

[a] Department of Orthopaedics, China-Japan Union Hospital of Jilin University,Changchun 130033, P. R. China. E-mail: zhongligao@sina.com
[b] Department of Orthopaedics, China-Japan Union Hospital of Jilin University,Changchun 130033, P. R. China. E-mail: lemonsean@163.com
[c] Department of Orthopaedics, China-Japan Union Hospital of Jilin University, Changchun 130033, P. R. China. E-mail: jlzuojianlin@163.com
[d] Department of Orthopaedics, China-Japan Union Hospital of Jilin University, Changchun 130033, P. R. China. E-mail: 342160503@qq.com
* Corresponding author

which isolated semi-round equiaxed intermetallic hexagonal (Ti, $Zr)_2Si$(S2) grains were dispersed within a continuous body-centered cubic(bcc) β-Ti matrix. Both phases were composed of ultrafine grains of several hundred nm. Similar to the Ti6Al4V alloy, the $(Ti\text{-}35Nb\text{-}7Zr\text{-}5Ta)_{98}Si_2$ alloy exhibited low cytotoxicity towards L-929 fibroblasts and allowed effective MC3T3-E1 osteoblast attachment with no significant effects on cell differentiation, inflammatory response, apoptosis or biomineralization.

Conclusion: This study demonstrates that the newly reported β-type titanium alloy $(Ti\text{-}35Nb\text{-}7Zr\text{-}5Ta)_{98}Si_2$, which has been reported to exhibit improved mechanical properties displays excellent biocompatibility. Therefore, this alloy may be a superior implant material in biomedical implantation.

Key words: β-Type Titanium Alloy; d-electron alloy design theory; spark plasma sintering; biocompatibility evaluation; cell differentiation

Introduction

Titanium and titanium alloys have been widely used as orthopedic implant materials due to their excellent mechanical strength and biocompatibility[1, 2]. However, higher elastic modulus of titanium alloys over the human bone can cause stress-shielding, leading to boneresorption[3-5]. Second-generation titanium alloys contain elements that can effectively enhance fabrication property and strength(e.g. Al, V);however, these constituent elements exhibit cytotoxicity [6]. Third-generation titanium alloys that contain biocompatible elements such as Ti, Zr, Nb, Ta, Si, and Sn

RSC Advances Accepted Manuscript

exhibit low elastic modulus close to that of the human bone[7]. In addition, these alloys demonstrate enhanced strength, plasticity, and good wear resistance properties suitable for use in biomedical implantation[8-12].

Compared with its coarse-grained counterparts, ultrafine-grained (UFGed) titanium and titanium alloys demonstrate higher wear resistance[13] and improved osteoblast adhesion[14]. It has been reported that wear loss of the UFGed TiNbZrTaFe alloy is only 3.5% and 1% of biomedical Ti6Al4V and Ti13Nb13Zr alloys, respectively[13, 15]. The d-electron alloy design theory developed by Morinaga *et al*. in 1988[16] has been successfully used to design biomedical titanium alloys with low elastic modulus[17-20]. Recently, Li *et al*. reported a new β-type titanium alloy$(Ti\text{-}35Nb\text{-}7Zr\text{-}5Ta)_{98}Si_2$, which was designed using the d-electron alloy design theory[21]. This alloy is a ductile UFGed alloy fabricated by spark plasma sintering (SPS) of nanocomposite powder precursor. It exhibits an excellent combination of low elastic modulus, ultra-large ductility, and high strength; and thus, biomechanically outperforms conventional α and β type titanium alloys[21]. Specifically, this new titanium alloy exhibits a low compressive elastic modulus of 35-40 GPa, an ultra-large fracture strain of 58-66%, as well as a high yield strength of 1,143-1,347 MPa and high fracture strength of 2,793-3,267 MPa. These results suggest the enormous potential of this alloy in biomedical use. However, the biocompatibility of the $(Ti\text{-}35Nb\text{-}7Zr\text{-}5Ta)_{98}Si_2$ alloy remains unreported.

In this study, we examined the microstructure of the $(Ti\text{-}35Nb\text{-}7Zr\text{-}5Ta)_{98}Si_2$ alloy by scanning electron microscopy (SEM). We then evaluated its biocompatibility

RSC Advances Accepted Manuscript

in vitro in the context of fibroblast cell proliferation and osteoblast cell adhesion, morphology, apoptosis, differentiation, inflammatory response, and biomineralization. The commercial titanium alloy Ti6Al4V was tested for side-by-side comparison.

Materials and Methods

Preparation of the (Ti-35Nb-7Zr-5Ta)$_{98}$Si$_2$alloy

The (Ti-35Nb-7Zr-5Ta)$_{98}$Si$_2$ alloy was prepared by Dr. Li, as previously described [21]. Briefly, high-purity powders of Ti (>99.7% pure, particle size<48 μm), Nb(>99.95% pure, particle size<45 μm), Zr (>99.5% pure, particle size<48 μm), Ta(>99.95% pure, particle size<45 μm), and Si (>99.99% pure, particle size<45 μm) were blended in a mechanical mixer for four hours at a rotation rate of 100 r/min. The mixture was subsequently loaded into a QM-2SP20-CL high-energy planetary ball milling system with a stainless steel ball to powder weight ratio of 10:1. High-energy ball milling was carried out at a rotation rate of 4.1 S^{-1} under the protection of purified argon gas. After milling, the powder samples were packed into a graphite die and sintered on an SPS-825 system (Sumitomo Coal Mining Co. Ltd, Tokyo, Japan). The alloy was sintered at 1,233K for five minutes in vacuum under a pressure of 50 MPa.

Microstructure of the (Ti-35Nb-7Zr-5Ta)$_{98}$Si$_2$ alloy

The microstructure of the alloy (Ti-35Nb-7Zr-5Ta)$_{98}$Si$_2$ prepared as above was examined by SEM (FEI, USA).

RSC Advances Accepted Manuscript

Surface characterization

The alloy samples were mirror polished using No. 400, 600, 800, and 1500 sandpaper, in that order. Surface characterization was conducted by SEM (JSM, Japan).

Cell culture

Mouse embryonic osteoblast MC3T3-E1 and mouse fibroblast L-929 cell lines were obtained from the cell bank of Chinese Academy of Sciences. MC3T3-E1 cells were cultured in DMEM/F12, while L-929 cells were cultured in PRMI 1640 medium; and both were cultured in a humidified incubator (100% humidity) with 5% CO_2at 37°C. Both DMEM/F12 and PRMI 1640 media were supplemented with 10% fetal calf serum(FCS) and 1% penicillin/streptomycin.

Cell proliferation and viability

Effects of alloys on the proliferation and viability of L-929 fibroblasts were evaluated by MTT assay *in vitro*. The $(Ti\text{-}35Nb\text{-}7Zr\text{-}5Ta)_{98}Si_2$ and commercial Ti6Al4V alloys were soaked in acetone and absolute ethyl alcohol for 20 minutes, followed by sterilization with0.15 MPa at 121°C for 40 minutes. After sterilization, samples were soaked in culture medium at 37°C for 24 hours at an optimized extraction ratio of $3cm^2/ml$ to generate the leaching liquor. L-929 cells in the logarithmic growth phase were suspended in the $(Ti\text{-}35Nb\text{-}7Zr\text{-}5Ta)_{98}Si_2$ or Ti6Al4V leaching liquor at 5×10^5 cells/ml and added into 96-well plates (200 μl/well). A

RSC Advances Accepted Manuscript

culture medium with 0.6% phenol was used as the positive control, and an ordinary culture medium was used as the negative control. After incubation in 5% CO_2at 37℃ for one, two, three, five or seven days, 20 μl of MTT solution (5mg/ml) was added into each well; and cells were incubated for four hours. The medium was replaced with 150 μl of dimethyl sulfoxide (DMSO) and absorbance was recorded on a spectrophotometer at 490 nm. Cell morphology was examined under a contrast microscope. Relative growth rate(RGR) was calculated using the equation:

$$\mathrm{RGR} = \frac{OD_E}{OD_N}$$

OD_E: optical density of the test group; OD_N: optical density of the negative group.

All experiments were performed in five replicates.

Cell attachment

Cell attachment was evaluated using the acridine orange(OA) staining method. MC3T3-E1 mouse embryonic osteoblasts were seeded at 1×10^5 cells/ml (3ml/well) into six-well plates containing sterilized $(Ti\text{-}35Nb\text{-}7Zr\text{-}5Ta)_{98}Si_2$ or Ti6Al4V alloy samples with a dimension of φ20×1 mm. After incubation at 37°C for one, three or six hours, alloy samples were collected, washed three times with PBS, and fixed in 95% ethanol for 15 minutes. After air-drying, the samples were soaked in 1% acetic acid for 30 seconds and stained with 0.01% OA for one minute. After washing three times with PBS, the samples were soaked in 0.1 M of $CaCl_2$for two minutes, washed three times with PBS, and subjected to fluorescence microscopic examination (100×).

RSC Advances Accepted Manuscript

Adherent cells were counted in five randomly selected fields. All experiments were performed in triplicates.

Cell morphology

MC3T3-E1 mouse embryonic osteoblasts were seeded at 1×10^7 cells/ml in six-well plates containing sterilized $(Ti\text{-}35Nb\text{-}7Zr\text{-}5Ta)_{98}Si_2$ or Ti6Al4V alloy samples with a dimension of φ20×1 mm. After incubation in 5% CO_2 at 37°C for three days, samples were collected, fixed in 2.5% glutaraldehyde for two hours, and fixed in 1% osmium tetroxide for two hours at 4°C. Fixed cells were dehydrated in a graded alcohol series and underwent critical-point drying. After gold sputtering, cells were examined under a SEM (Hitachi, Japan) equipped with a semiautomatic interactive image analyzer. All experiments were conducted in triplicates.

Cell differentiation and inflammatory response

Effects of alloys on MC3T3-E1 embryonic osteoblast differentiation and inflammatory response were evaluated based on the concentration of alkaline phosphatase (ALP) and interleukin-6 (IL-6) in the cell culture, respectively. MC3T3-E1 cells were seeded at 1×10^5 cells/ml into 24-well plates containing sterilized $(Ti\text{-}35Nb\text{-}7Zr\text{-}5Ta)_{98}Si_2$ or Ti6Al4V alloy samples with a dimension of φ10×1 mm. Cells cultured in the absence of alloys were used as the negative control. After incubation in 5% CO_2 at 37°C for one, three or six days, 50μL of culture medium samples were collected; and the concentration of ALP and IL-6 were

RSC Advances Accepted Manuscript

determined using ELISA kits from Beyotime (Beijing, China), according to manufacturer's instructions. All experiments were conducted in triplicates.

Biomineralization

Biomineralization was evaluated using the alizarin red staining method. Briefly, MC3T3-E1 mouse embryonic osteoblasts were seeded at 1×10^4 cells/ml in 24-well plates containing sterilized $(Ti\text{-}35Nb\text{-}7Zr\text{-}5Ta)_{98}Si_2$ or Ti6Al4V alloy samples with a dimension of φ10×1 mm. After 24 h incubation, the culture medium was replaced with mineralized culture medium (DMEM/F12 supplemented with 10% FCS, 1% penicillin/streptomycin, 10 mmol/l sodium glycerol phosphate, 0.1 μmol/l dexamethasone, and 50 mg/l vitamin C). The mineralized culture medium was replaced every three days. On day 30, the samples were collected, washed thrice in PBS, fixed in 4% paraformaldehyde for 30 min, and stained with 40 mmol/l alizarin red (sigma) for 20 min. Calcium deposits in mineralized nodules were examined by xxxx. The stain was extracted in 10% cetyl pyridinium chloride (sigma). Absorbance at 590 nm was recorded on a spectrophotometer.

Cell apoptosis

Effects of alloys on cell apoptosis were studied using an Annexin V-FITC cell apoptosis detection kit from Beyotime (Beijing, China). Briefly, MC3T3-E1 mouse embryonic osteoblasts were seeded at 1×10^7 cells/ml into six-well plates containing sterilized $(Ti\text{-}35Nb\text{-}7Zr\text{-}5Ta)_{98}Si_2$ or Ti6Al4V alloy samples with a dimension

RSC Advances Accepted Manuscript

ofφ20×1 mm. Cells cultured in the absence of alloy samples were used as the negative control. After incubation in 5% CO_2 at 37°Cfor 24 hours, alloy samples were separated from the culture medium. The samples were washed once with PBS and treated with trypsin. After trypsin was removed, adherent cells were suspended in culture medium and centrifuged twice at 1,000×g for five minutes. Cell pellets were resuspended in 195 μl of Annexin V-FITC binding buffer. After the addition of 5 μl of Annexin V-FITC and 10 μl of propidium iodide(PI), cells were incubated at room temperature for 20 minutes and subjected to analysis on a flow cytometer (Beckman Coulter, USA). All experiments were conducted in triplicates.

Statistical Analysis

Results are presented as mean ± standard deviation (SD). Differences between treatment groups were analyzed using one-way analysis of variance (ANOVA). Differences with $P<0.05$ were considered statistically significant.

Results

Microstructure of the (Ti-35Nb-7Zr-5Ta)$_{98}$Si$_2$ alloy

RSC Advances Accepted Manuscript

The SEM micrograph of the $(Ti\text{-}35Nb\text{-}7Zr\text{-}5Ta)_{98}Si_2$ alloy is shown in Figure 1. The alloy displayed a homogeneous two-phase microstructure, in which isolated semi-round equiaxed intermetallic hexagonal $(Ti, Zr)_2Si$(S2) grains were dispersed within a continuous body-centered cubic(bcc) β-Ti matrix. This two-phase

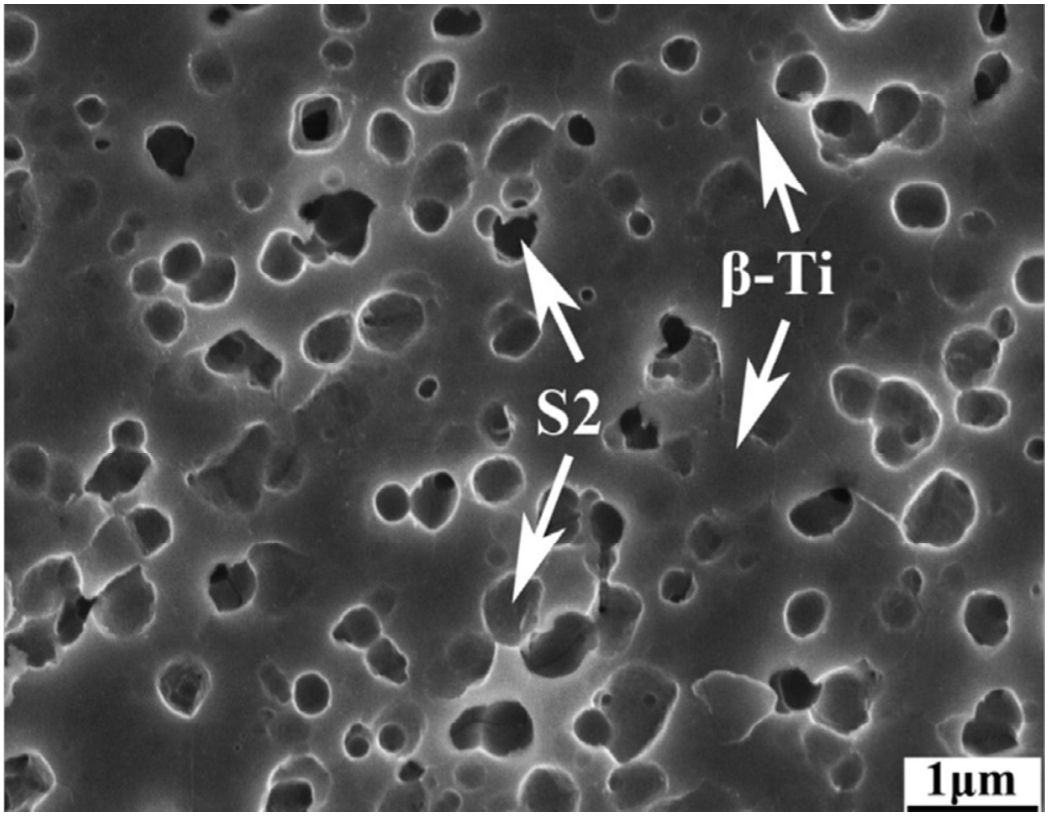

microstructure is distinct from that of the $Ti_{60}Zr_{10}Nb_{15}Si_{15}$ (at.%) alloy fabricated by cast method, in which a homogeneous hexagonal$(Ti, Zr)_5Si_3$(S1) primary phase was embedded in a dendritic S1+β-Ti eutectic matrix[10]. Moreover, both the bcc β-Ti andS2 phases in the $(Ti\text{-}35Nb\text{-}7Zr\text{-}5Ta)_{98}Si_2$ alloy displayed ultra-fine grains of several hundred nm.

Figure 1.SEM micrographof the $(Ti\text{-}35Nb\text{-}7Zr\text{-}5Ta)_{98}Si_2$ alloy.β-Ti: β-Ti matrix, S2: $(Ti, Zr)_2Si$ phase.

RSC Advances Accepted Manuscript

Surface characterization

Surface characterization of the alloys was conducted by SEM. As showed in Figure 2, the polished samples of both $(Ti\text{-}35Nb\text{-}7Zr\text{-}5Ta)_{98}Si_2$ and Ti6Al4V alloys displayed a glossy surface with scratches in the same direction. There were no notable differences between the two alloys.

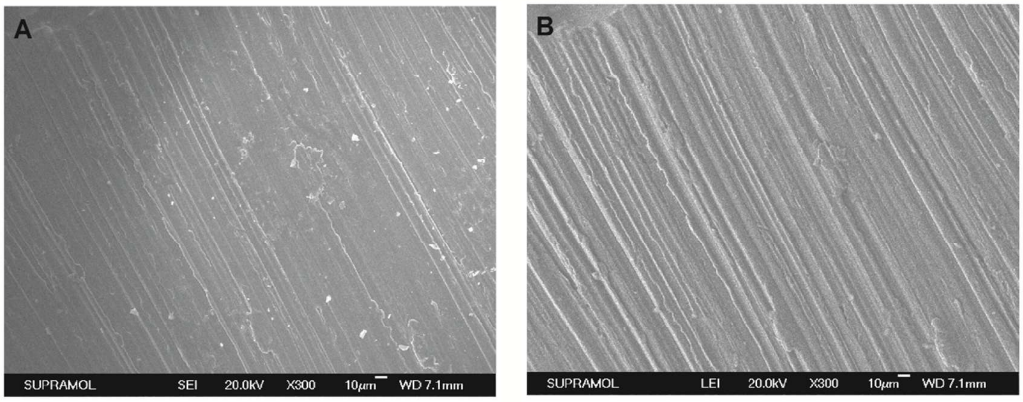

Figure 2. Surface SEM observation of the Ti6Al4V and $(Ti\text{-}35Nb\text{-}7Zr\text{-}5Ta)_{98}Si_2$ alloys. (A)Ti6Al4V. (B): $(Ti\text{-}35Nb\text{-}7Zr\text{-}5Ta)_{98}Si_2$.

Cell proliferation and viability

Effects of the $(Ti\text{-}35Nb\text{-}7Zr\text{-}5Ta)_{98}Si_2$ and commercial Ti6Al4V alloys on the proliferation and viability of L-929 mouse fibroblasts *in vitro* up to seven days were evaluated by MTT assay. Cells cultured in the leaching liquors of these two alloys were found to have very similar overall growth curves to that of cells in normal culture medium (Fig. 3). Significant differences were observed only on day five, when cells in both leaching liquors revealed a significantly lower viability than the negative control (Fig. 3B). However, cells in the $(Ti\text{-}35Nb\text{-}7Zr\text{-}5Ta)_{98}Si_2$ leaching liquor revealed a significant higher viability than cells in the Ti6Al4V leaching liquor

RSC Advances Accepted Manuscript

on day five, suggesting the lower cytotoxicity of the $(Ti\text{-}35Nb\text{-}7Zr\text{-}5Ta)_{98}Si_2$ alloy. When examined under a contrast microscope, cells cultured in the two leaching liquors were morphologically similar to cells cultured in normal medium. The RGRs of cells cultured in the alloy leaching liquors are presented in Table 1. The cytotoxicity of the $(Ti\text{-}35Nb\text{-}7Zr\text{-}5Ta)_{98}Si_2$ alloy assessed by RGR is at level 0-1,according to ISO 10993-5 standard (level 0: RGR≥100%, level 1: 99%>RGR≥75%), which is generally considered safe.

RSC Advances Accepted Manuscript

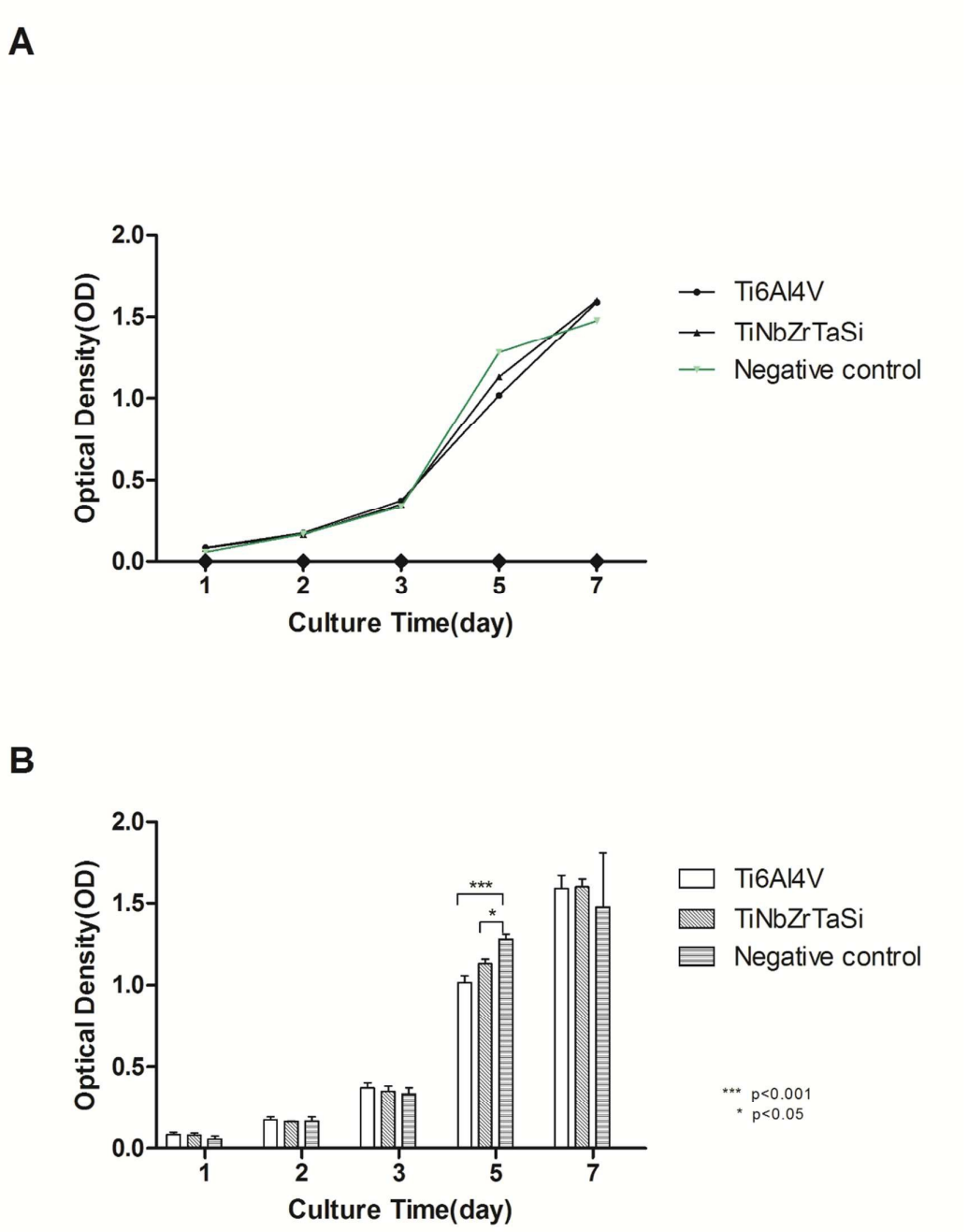

Figure 3 Proliferation and viability of L-929 mouse fibroblasts cultured in leaching liquors of the $(Ti\text{-}35Nb\text{-}7Zr\text{-}5Ta)_{98}Si_2$ and Ti6Al4V alloys and normal medium by MTT assay. n=5, *P<0.05, ***P<0.001.

Table 1.RGRs of L-929 mouse fibroblasts cultured in leaching liquors of $(Ti\text{-}35Nb\text{-}7Zr\text{-}5Ta)_{98}Si_2$ and Ti6Al4V alloys.

RSC Advances Accepted Manuscript

Group	Time				
	1d	2d	3d	5d	7d
$(Ti\text{-}35Nb\text{-}7Zr\text{-}5Ta)_{98}Si_2$	121.79%	97.38%	104.45%	88.29%	96.23%
Ti6Al4V	125.97%	103.81%	110.74%	79.43%	95.60%

Cell attachment

The attachment of MC3T3-E1 mouse embryonic osteoblasts to $(Ti\text{-}35Nb\text{-}7Zr\text{-}5Ta)_{98}Si_2$ and Ti6Al4V alloys were assessed after co-incubation *in vitro* using the OA staining method. When excited with blue fluorescence, OA-stained live cells fluoresce green, while apoptotic cells fluoresce yellow-green. Fluorescence microscopic images of alloy-attached cells after one, three or six hours of co-incubation are shown in Figure 4. All adherent cells fluoresced green, indicating that these were all live cells. When the number of adherent cells was counted, no significant differences between the two alloys were detected (Fig. 5), suggesting that the $(Ti\text{-}35Nb\text{-}7Zr\text{-}5Ta)_{98}Si_2$ alloy has similar cell attachment properties to the Ti6Al4V alloy.

RSC Advances Accepted Manuscript

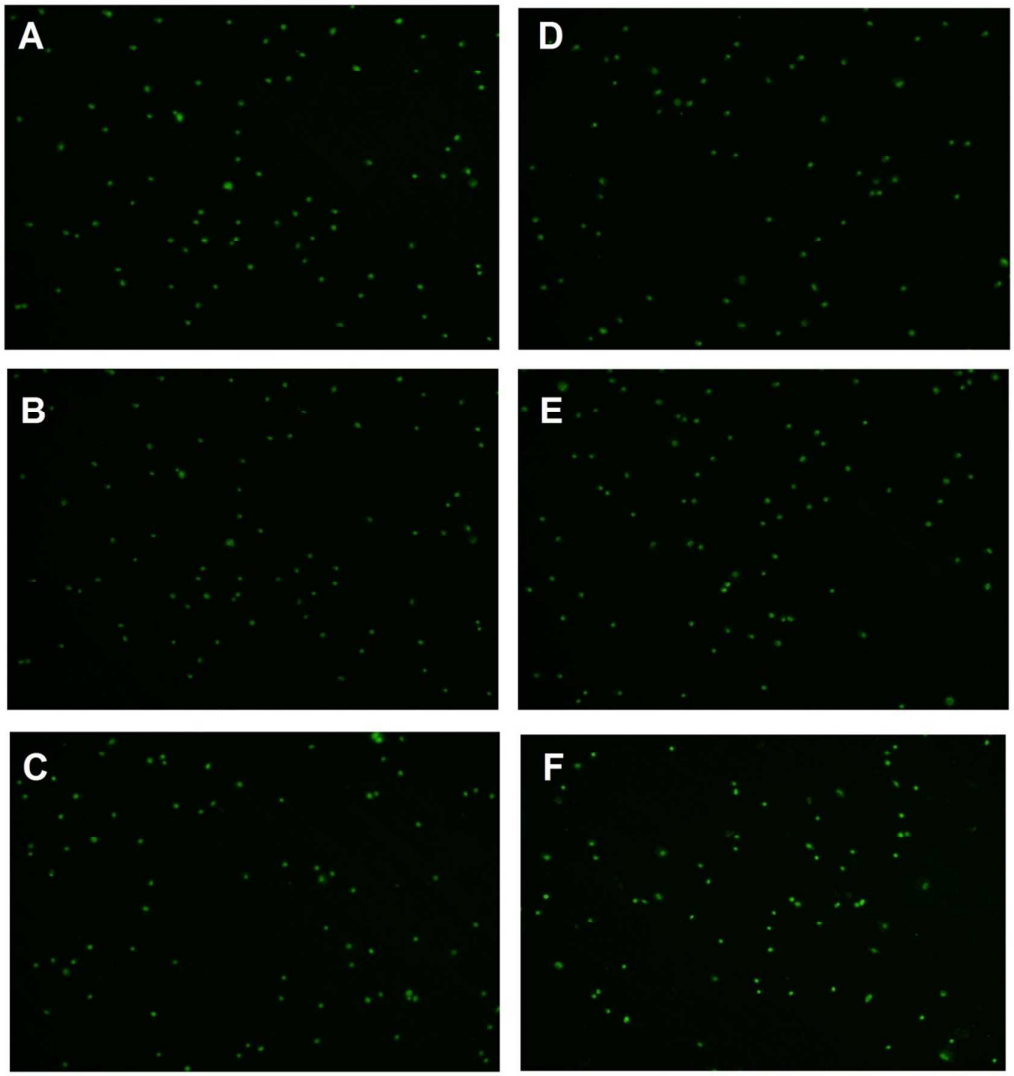

Figure 4 Fluorescence microscopic images of AO-stained, alloy-attached MC3T3-E1 mouse embryonic osteoblasts after co-incubation *in vitro*. (A-C)Cells attached to the Ti6Al4V alloy after one, three or six hours of co-incubation. (D-F)Cells attached to the $(Ti\text{-}35Nb\text{-}7Zr\text{-}5Ta)_{98}Si_2$ alloy after one, three or six hours of co-incubation.

RSC Advances Accepted Manuscript

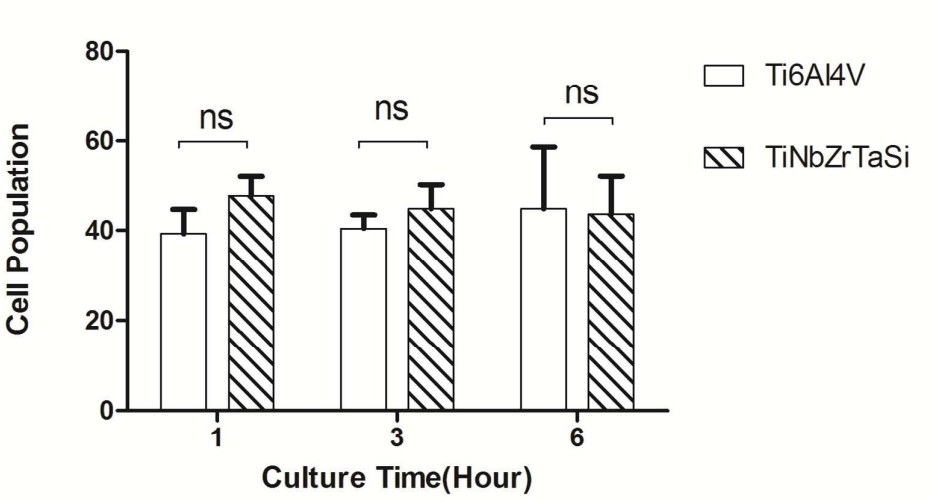

Figure 5 The number of MC3T3-E1 mouse embryonic osteoblasts that attached to the (Ti-35Nb-7Zr-5Ta)$_{98}$Si$_2$or Ti6Al4V alloy after one, three or six hours of co-incubation *in vitro* by the AO staining method. *n*=3, ns means nonspecific (*P*>0.05).

Cell morphology

Cell morphology of MC3T3-E1 mouse embryonic osteoblasts that attached to the (Ti-35Nb-7Zr-5Ta)$_{98}$Si$_2$ or Ti6Al4V alloy after three days of co-incubation were examined by SEM. All adherent cells displayed an elongated morphology with cytoplasmic extension (Fig. 6). No notable differences in cell morphology were observed between the (Ti-35Nb-7Zr-5Ta)$_{98}$Si$_2$ and Ti6Al4V alloys.

RSC Advances Accepted Manuscript

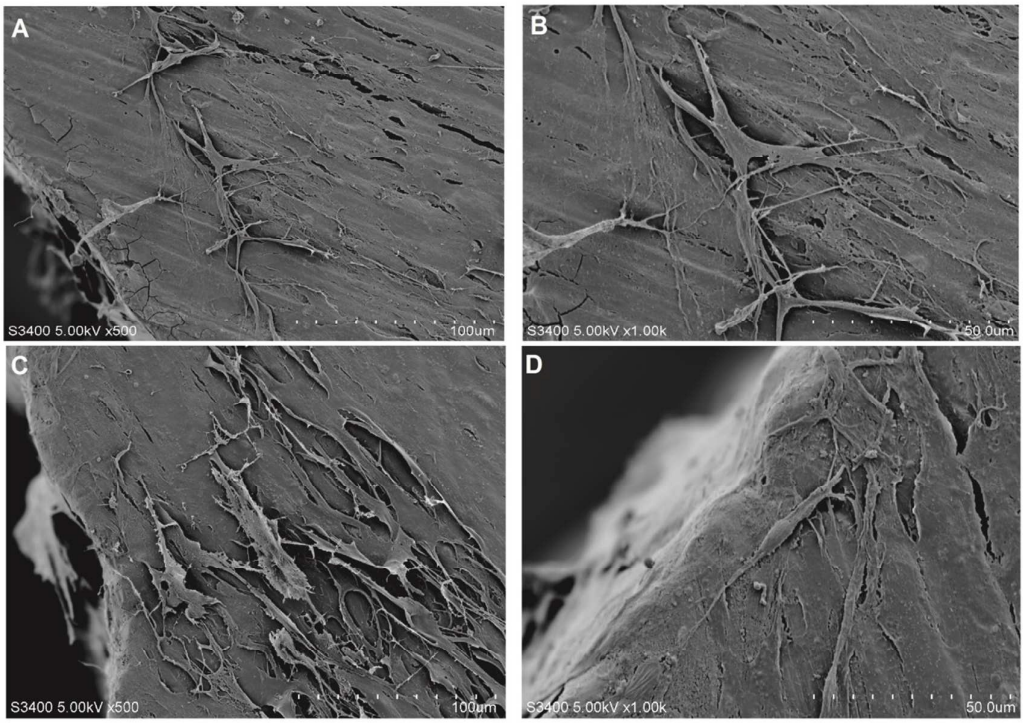

Figure 6 SEM images of MC3T3-E1 mouse embryonic osteoblasts that attached to the $(Ti\text{-}35Nb\text{-}7Zr\text{-}5Ta)_{98}Si_2$ or Ti6Al4V alloy after three days of co-incubation.(A-B)Cells that attached to the Ti6Al4V alloy are shown. (C-D) Cells that attached to the$(Ti\text{-}35Nb\text{-}7Zr\text{-}5Ta)_{98}Si_2$ alloy are shown.

Cell differentiation

ALP is a marker of osteoblast differentiation. Effects of alloys on MC3T3-E1 embryonic osteoblast differentiation were assessed based on ALP concentrations in culture medium. After MC3T3-E1 cells were co-cultured with the $(Ti\text{-}35Nb\text{-}7Zr\text{-}5Ta)_{98}Si_2$ or Ti6Al4V alloy for one, three or six days, no significant differences in ALP concentrations were detected between the two alloys (Fig. 7). Importantly, ALP concentrations in the culture medium of alloy-treated cells were similar to concentrations of the negative control ($P>0.05$), indicating that neither alloy promotes osteoblast differentiation.

RSC Advances Accepted Manuscript

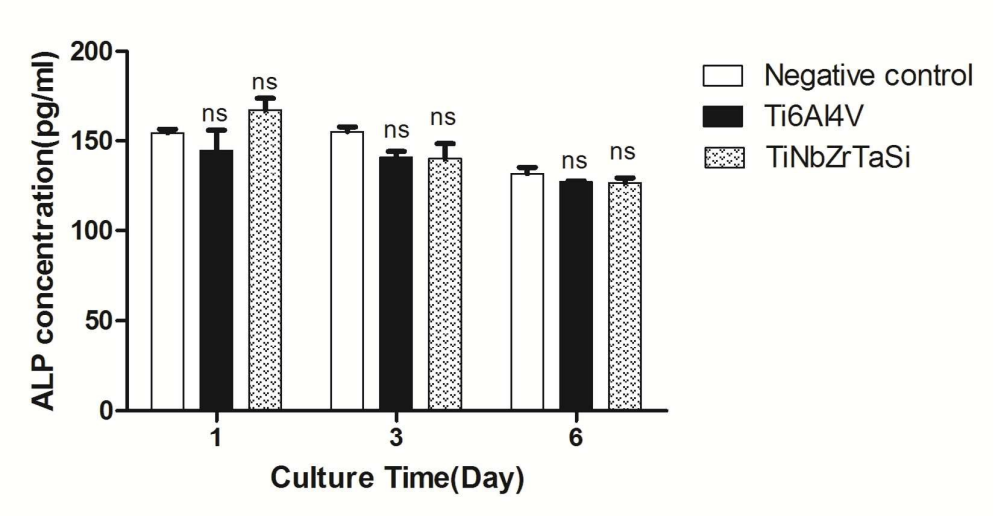

Figure 7 ALP concentrations in the culture medium of MC3T3-E1 embryonic osteoblasts cultured for one, three or six days in normal medium or medium containing the $(Ti\text{-}35Nb\text{-}7Zr\text{-}5Ta)_{98}Si_2$ or Ti6Al4V alloy. *n*=3, ns means nonspecific (*P*>0.05).

Inflammatory response

IL-6 is a well-recognized marker for cellular inflammatory response. Effects of alloys on MC3T3-E1 embryonic osteoblast inflammatory response were evaluated based on IL-6 concentrations in culture medium. No significant differences in IL-6 concentrations were detected between MC3T3-E1 cell cultures containing the $(Ti\text{-}35Nb\text{-}7Zr\text{-}5Ta)_{98}Si_2$ or Ti6Al4V alloy after one, three or six days of incubation, as shown in Figure 8. Moreover, IL-6 concentrations in the culture medium of alloy-treated cells were similar to concentrations in the culture medium of the negative control (*P*>0.05), indicating that neither alloy stimulates inflammatory response in osteoblasts.

RSC Advances Accepted Manuscript

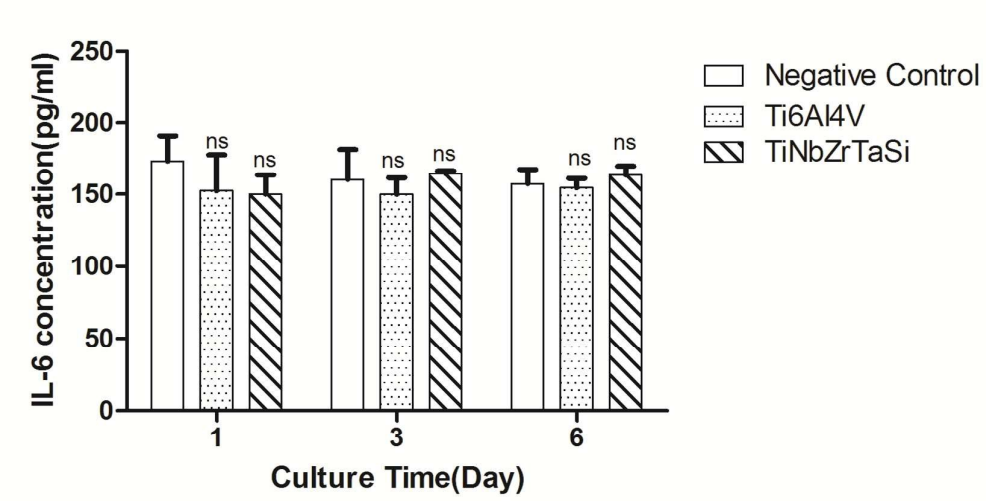

Figure 8 IL-6 concentrations in the culture medium of MC3T3-E1 embryonic osteoblasts cultured for one, three or six days in normal medium or medium containing the (Ti-35Nb-7Zr-5Ta)$_{98}$Si$_2$ or Ti6Al4V alloy. *n*=3, ns means nonspecific (*P*>0.05).

Biomineralization

Calcium deposits in osteoblasts are an indication of successful *in vitro* bone formation. In this study, calcium deposits in MC3T3-E1 embryonic osteoblasts formed mineralized nodules, which were stained bright orange-red with alizarin red S (Fig. 9). The stain was subsequently extracted in 10% cetyl pyridinium chloride and detected on a spectrophotometer (Fig. 10). While cells co-cultured with the Ti6Al4V or (Ti-35Nb-7Zr-5Ta)$_{98}$Si$_2$ alloy both showed significantly greater calcium deposition compared with negative control, no significant difference in biomineralization was detected between the two alloys.

RSC Advances Accepted Manuscript

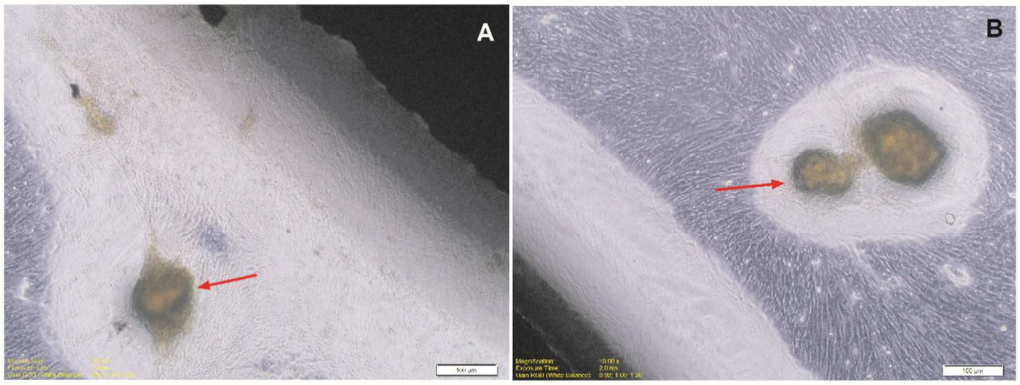

Figure 9 Mineralized nodules detected under an inverted microscope. MC3T3-E1 embryonic osteoblasts were co-cultured with the Ti6Al4V (A) or $(Ti\text{-}35Nb\text{-}7Zr\text{-}5Ta)_{98}Si_2$ (B) alloy for 30 days..

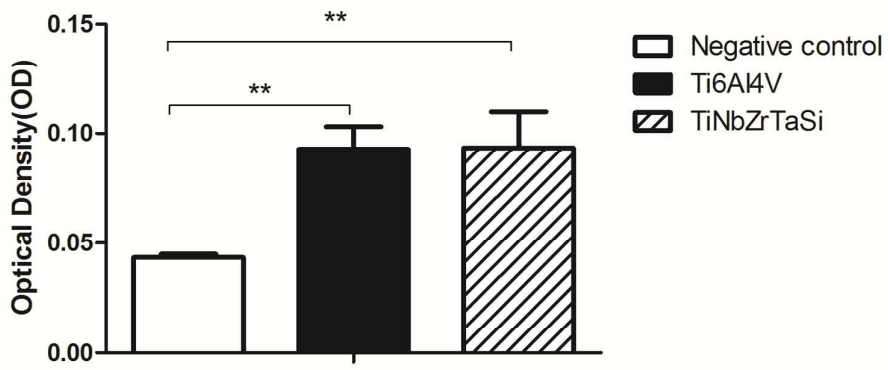

Figure 10 Biomineralization of MC3T3-E1 embryonic osteoblasts. Cells were co-cultured with the $(Ti\text{-}35Nb\text{-}7Zr\text{-}5Ta)_{98}Si_2$ alloy, the Ti6Al4V alloy, or negative control for 30 days. Calcium deposition was determined by the alizarin red staining method. n=3, $^{**}P<0.01$.

Cell apoptosis

Effects of alloys on cell apoptosis were studied using the Annexin V-FITC cell apoptosis assay. MC3T3-E1 mouse embryonic osteoblasts were cultured in normal medium or medium containing the $(Ti\text{-}35Nb\text{-}7Zr\text{-}5Ta)_{98}Si_2$ or Ti6Al4V alloy for 24 hours. Cells that attached to the alloys were dissociated, resuspended in medium, and subjected to flow cytometric analysis. As shown in Figure 11, quadrants B4 and B2

RSC Advances Accepted Manuscript

represent the percentage of early and late-stage apoptotic cells, while quadrants B3 and B1 represent live and necrotic cells, respectively. No significant difference in the total number of apoptotic cells was detected between cells that attached to the $(Ti\text{-}35Nb\text{-}7Zr\text{-}5Ta)_{98}Si_2$ or the Ti6Al4V alloy, or cells cultured in normal medium(P>0.05, Fig. 12), indicating that neither alloy activates cell apoptosis in osteoblasts.

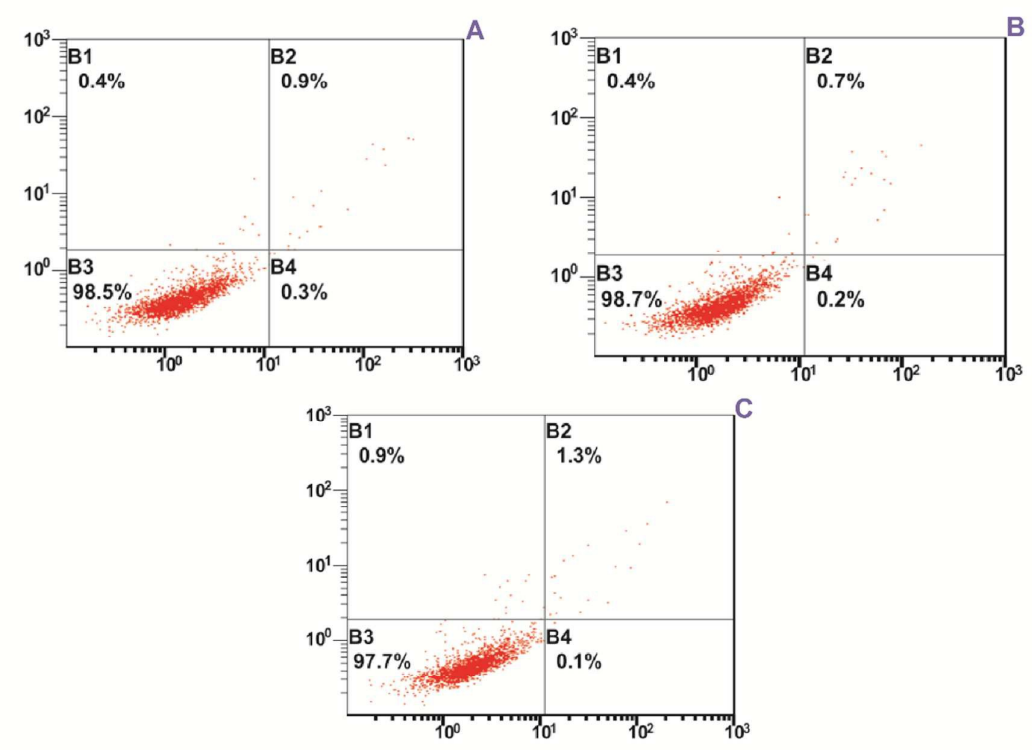

Figure 11 Apoptosis rate of MC3T3-E1 mouse embryonic osteoblastsby flow cytometry using the Annexin V-FITC cell apoptosis assay.(A)Cells cultured in normal medium for 24 hours. (B)Cells attached to the Ti6Al4V alloy after 24 hours of co-incubation. (C) Cells attached to the $(Ti\text{-}35Nb\text{-}7Zr\text{-}5Ta)_{98}Si_2$ alloy after 24 hours of co-incubation.

RSC Advances Accepted Manuscript

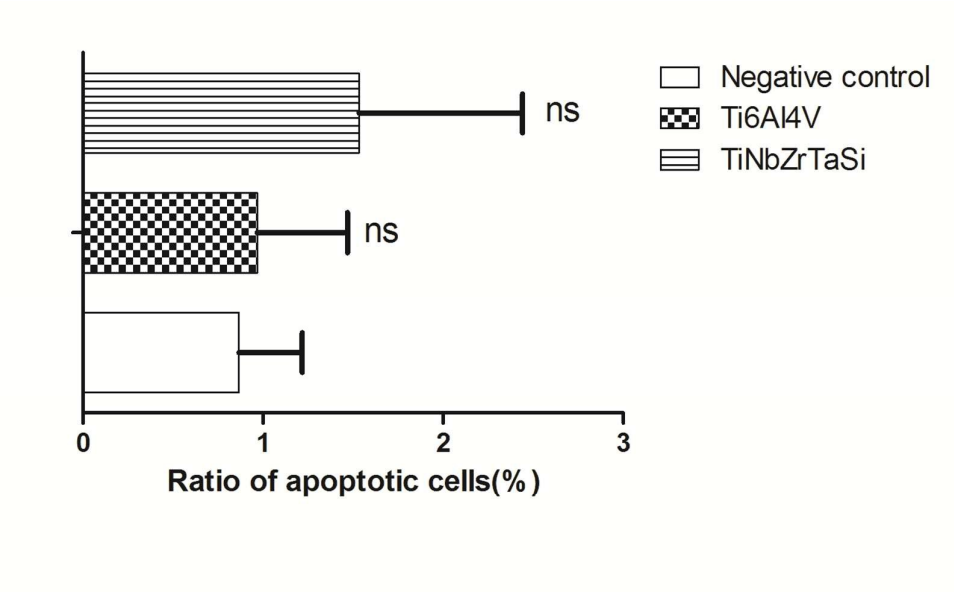

Figure 12 Apoptosis rate of MC3T3-E1 mouse embryonic osteoblasts by flow cytometry. *n*=3, ns means nonspecific (*P*>0.05).

Discussion

The higher elastic modulus of metallic implants over the human bone can cause bone reduction around the implants, and eventually lead to implant looseness and fracture. Titanium and its alloys are widely used as implant materials for their excellent biocompatibility. However, theTi6Al4V alloy, which is the most commonly used titanium alloy in biomedical implantation, exhibits high elastic modulus. In addition, the constituent element V in the alloy can cause tissue inflammation and even tumor formation, and the element Al can cause chronic tissue impairment[22]. β-Type titanium alloys, which contain β phase stable elements such as Nb, Pd, Ta, Zr, Mo, Sn, and Fe exhibit a favorable combination of good biocompatibility and reduced elastic modulus compared with Ti6Al4V[23, 24]. The recently reported β-type

RSC Advances Accepted Manuscript

titanium alloy $(Ti\text{-}35Nb\text{-}7Zr\text{-}5Ta)_{98}Si_2$ displays a low elastic modulus of 37GPa, which is close to that of the human bone[21]. However, the microstructure and biocompatibility of this alloy remains unreported.

In this study, we first examined the microstructure of the $(Ti\text{-}35Nb\text{-}7Zr\text{-}5Ta)_{98}Si_2$ alloy by SEM. We found that this alloy exhibits a two-phase microstructure, in which isolated semi-round equiaxed intermetallic hexagonal $(Ti, Zr)_2Si$(S2) grains were dispersed within a continuous bccβ-Ti matrix. Ultrafine grains of several hundred nm were detected in both phases. These unique microstructural features might be responsible forthe enhanced strength and ultra-large ductility of this alloy. This alloy has been reported to crack preferentially in the fragile S2 region under compressive stress[21],which would prevent cracks into the bcc β-Ti matrix and delay the propagation of dislocations and dislocation multiplication[25-27].

We subsequently studied the comparative biocompatibility of this alloy in the context of *in vitro* cell cytotoxicity, cell attachment, cell morphology, cell differentiation and inflammatory response, cell apoptosis, and biomineralization. Our MTT assay results revealed that L-292 mouse fibroblasts cultured in leaching liquors of the $(Ti\text{-}35Nb\text{-}7Zr\text{-}5Ta)_{98}Si_2$ or Ti6Al4V alloy for up to seven days proliferated at rates similar to cells in normal medium. Compared with cells in normal medium, cells cultured in alloy leaching liquors exhibited a significantly reduced viability only on day five. Moreover, cells in the $(Ti\text{-}35Nb\text{-}7Zr\text{-}5Ta)_{98}Si_2$ leaching liquor displayed a higher viability than cells in the Ti6Al4V leaching liquor on day five. These results suggest that the cytotoxicity of the $(Ti\text{-}35Nb\text{-}7Zr\text{-}5Ta)_{98}Si_2$ alloy is as low as that of

RSC Advances Accepted Manuscript

the commercial Ti6Al4V alloy, if not lower.

Inadequate osteoblast adhesion can result in implant destabilization, as well as impaired bone tissue repair and regeneration, leading to implant failure[28]. In this study, we assessed the osteoblast adhesion properties of the $(Ti\text{-}35Nb\text{-}7Zr\text{-}5Ta)_{98}Si_2$and Ti6Al4V alloys using the OA staining method. After MC3T3-E1 mouse embryonic osteoblasts were co-incubated with the $(Ti\text{-}35Nb\text{-}7Zr\text{-}5Ta)_{98}Si_2$ or Ti6Al4V alloy for one, three or six hours, no significant difference in cell attachment between these two alloys was detected, suggesting that osteoblasts can effectively adhere to the $(Ti\text{-}35Nb\text{-}7Zr\text{-}5Ta)_{98}Si_2$ alloy within a short period of time. Furthermore, fluorescence imaging indicated that all alloy-attached cells were live cells. When examined by SEM, alloy-attached cells after three days of co-incubation displayed an elongated morphology with cytoplasmic extension; and no notable differences were detected between the two alloys. Moreover, the apoptosis rates of cells that attached to both alloys were as low as cells cultured in normal medium, further underscoring the low cytotoxicity of the $(Ti\text{-}35Nb\text{-}7Zr\text{-}5Ta)_{98}Si_2$ alloy.

Biomedical implants may potentially affect osteoblast differentiation and/or elicit an immune response that can either sustain regeneration or lead to fibrosis in case of an aggravated inflammation[29]. Thus, we evaluated the effects of the $(Ti\text{-}35Nb\text{-}7Zr\text{-}5Ta)_{98}Si_2$ and Ti6Al4V alloys on MC3T3-E1 embryonic osteoblast differentiation and inflammatory response by determining the levels of ALP and IL-6 in cell culture using ELISA. After one, three, and six days of incubation, no

RSC Advances Accepted Manuscript

significant differences in either ALP or IL-6 concentrations were detected between the two alloy-treated cell cultures, or between any alloy-treated cell culture and normal cell culture. These results indicate that the $(Ti\text{-}35Nb\text{-}7Zr\text{-}5Ta)_{98}Si_2$ alloy, like the commercial Ti6Al4V alloy, does not stimulate differentiation or elicit an immune response in osteoblasts.

Biomineralization of osteoblasts is the initial step of bone formation. Quick bone formation helps increase the stability of the implanted metal prosthesis. Our results showed that, after 30 d incubation in mineralized culture medium, MC3T3-E1 embryonic osteoblasts co-cultured with the Ti6Al4V or $(Ti\text{-}35Nb\text{-}7Zr\text{-}5Ta)_{98}Si_2$ alloy displayed greater calcium deposition compared with cells cultured in the absence of alloy. Importantly, no significant difference in biomineralization was detected between the two alloys. These results indicate that the $(Ti\text{-}35Nb\text{-}7Zr\text{-}5Ta)_{98}Si_2$ alloy is as effective as the Ti6Al4V alloy in promoting osteoblast biomineralization.

Conclusion

The novel β-type titanium alloy $(Ti\text{-}35Nb\text{-}7Zr\text{-}5Ta)_{98}Si_2$ exhibits a unique two-phase microstructure, which is possibly responsible for its excellent strength and plasticity. In regard to its biocompatibility, this alloy displays low cytotoxicity similar to the commercial Ti6Al4V alloy, if not lower. Moreover, similar to the Ti6Al4V alloy, this novel titanium alloy allows effective osteoblast adhesion with no significant impact on cell differentiation, apoptosis, inflammatory response, and biomineralization. Therefore, the $(Ti\text{-}35Nb\text{-}7Zr\text{-}5Ta)_{98}Si_2$ alloy displays both excellent

RSC Advances Accepted Manuscript

mechanical properties and biocompatibility, suggesting that it may be a superior implant material for biomedical application.

Acknowledgement

The authors are grateful for the financial support from Jilin University (project 3R113U763430) and Graduate Innovation Fund of Jilin University (project 2015015).

References

1. Yoshimitsu Okazaki, E.N., Hiroshi Nakada, Kihei Kobayash, *Surface analysis of Ti-15Zr-4Nb-4Ta alloy after implantation in rat tibia.* Biomaterials, 2001. **22**: p. 599-607.
2. Kulkarni, M., et al., *Titanium nanostructures for biomedical applications.* Nanotechnology, 2015. **26**(6): p. 062002.
3. X.J.Wang, Y.C.L., J.Y. Xiong,P.D.Hodgson,C.E. Wen, *PorousTiNbZr alloy scaffolds for biomedical applications.* Acta Biomater, 2009. **5**: p. 3616-3624.
4. Niinomi, M., *Mechanical properties of biomedical titanium alloys.* Mater. Sci. Eng. A, 1998. **243**: p. 231-236.
5. I.H. Oh, N.N., N. Masahashi, S. Hanada, *Mechanical properties of porous titanium compacts prepared by powder sintering.* Scr. Mater, 2003. **49**: p. 1197-1202.
6. Hanawa, T., *Recent development of new alloys for biomedical use.* Mater. Sci. Forum, 2006. **512**: p. 243-248.
7. Evans, F.G., *The mechanical properties of bone.* Artif. Limbs, 1969. **13**: p. 37-48.
8. Y.H. Li, C.Y., H.D. Zhao, S.G. Qu, X.Q. Li, Y.Y. Li, *New developments of Ti-Based alloys for biomedical applications.* Materials, 2014. **7**: p. 1709-1800.
9. V.Brailovski, S.P., M. Gauthier, K.Inaekyan,S.Dubinskiy,M.Petrzhik, etal., *Bulk and porous metastable beta Ti-Nb-Zr (Ta) alloys for biomedical applications.* Mater. Sci. Eng. C, 2011. **31**: p. 643-657.
10. S. Abdi, M.S.K., O. Shuleshova, M. Bönisch, M. Calin, L. Schultz, et al., *Effect of Nb addition on microstructure evolution and nanomechanical properties of a glass-forming Ti-Zr-Si alloy.* Intermetallics, 2014. **46**: p. 156-163.
11. M. Geetha, A.K.S., R. Asokamani, A.K. Gogia, *Ti based biomaterials, the*

RSC Advances Accepted Manuscript

ultimate choice for orthopaedic implant — a review. Prog. Mater. Sci, 2009. **54**: p. 397-425.

12. H. Matsumoto, S.W., S.J. Hanada, *Beta TiNbSn alloys with low Young's modulus and high strength.* Mater. Trans., 2005. **46**: p. 1070-1078.
13. L.M. Zou, L.J.Z., C. Yang, S.G. Qu, Y.Y. Li, *Unusual dry sliding tribological behavior of biomedical ultrafine-grained TiNbZrTaFe composites fabricated by powder metallurgy.* J. Mater. Res., 2014. **29**: p. 902-909.
14. T.J. Webster, J.U.E., *Increased osteoblast adhesion on nanophase metals: Ti, Ti6Al4V, and CoCrMo.* Biomaterials, 2004. **25**: p. 4731-4739.
15. Y.Y. Li, L.M.Z., C. Yang, Y.H Li, L.J. Li, *Ultrafine-grained Ti-based composites with high strength and low modulus fabricated by spark plasma sintering.* Mater. Sci. Eng. A, 2013. **560**: p. 857-861.
16. M. Morinaga, N.Y., T. Maya, K. Sone, H. Adachi, *Theoretical design of titanium alloys*, in *The Sixth World Conference on Titanium*. 1988: Cannes. p. 1601-1606.
17. Y.L. Zhou, M.N., T. Akahori, *Effects of Ta content on Young's modulus and tensile properties of binary Ti-Ta alloys for biomedical applications.* Mater. Sci. Eng. A, 2004. **371**: p. 283-290.
18. Y. Li, X.P.S., *A study of low Young's modulus Ti-Nb-Zr alloys using d electrons alloy theory.* Scr. Mater, 2012. **67**: p. 57-60.
19. M. Abdel-Hady, K.H., M. Morinaga, *General approach to phase stability and elastic properties of beta-type Ti-alloys using electronic parameters.* Scr. Mater., 2006. **55**: p. 477-480.
20. D. Kuroda, M.N., M. Morinaga, Y. Kato, T. Yashiro, *Design and mechanical properties of new β type titanium alloys for implant materials.* Mater. Sci. Eng. A, 1998. **243**: p. 244-249.
21. Li, Y.H., et al., *Biomedical TiNbZrTaSi alloys designed by d-electron alloy design theory.* Materials & Design, 2015. **85**: p. 7-13.
22. Song Y.Xu D S, Y.R., Li D.et, *Theoretical Study of the Effects of Alloying Elements on the Strength and Modulus of β-type Biotitanium Alloys.* Mater Sci Eng, 1999. **A260**: p. 269-274.
23. Niinomi, M., *Recent research and development in titanium alloys for biomedical applications and healthcare goods.* Science and Technology of Advanced Materials, 2003. **4**: p. 445-454.
24. M.Niinomi, *Fatigue performance and cyto -toxicity of low rigidity titanium alloy, Ti-29Nb-13Ta-4.6Zr.* Biomaterials, 2003. **24**: p. 2673-2683.
25. Q.S. Wei, S.J.S., S.M. Zhu, G. Wang, J. Wang, M.S. Dargusch, *Compressive deformation behavior of a near-beta titanium alloy.* Mater. Des., 2012. **34**: p. 739-745.
26. G. Wang, Y.J.H., J. Shen, *Novel TiCuNiCo composites with high fracture strength and plasticity.* Mater. Des., 2012. **33**: p. 226-230.
27. L.H. Liu, C.Y., F. Wang, S.G. Qu, X.Q. Li, W.W. Zhang, et al., *Ultrafine grained Ti-based composites with ultrahigh strength and ductility achieved by equiaxing microstructure.* Mater. Des., 2015. **79**: p. 1-5.

RSC Advances Accepted Manuscript

28. L.C. Baxter, V.F., M. Textor, I. ap Gwynn, R.G. Richards, *Fibroblast and osteoblast adhesion and morphology on calcium phosphate surfaces.* Eur. Cell Mater., 2002. **4**: p. 1-17.
29. L. He, A.G.M., *Macrophages are essential for the early wound healing response and the formation of a fibrovascular scar.* Am. J. Pathol., 2013. **182**: p. 2407-2417.

RSC Advances Accepted Manuscript

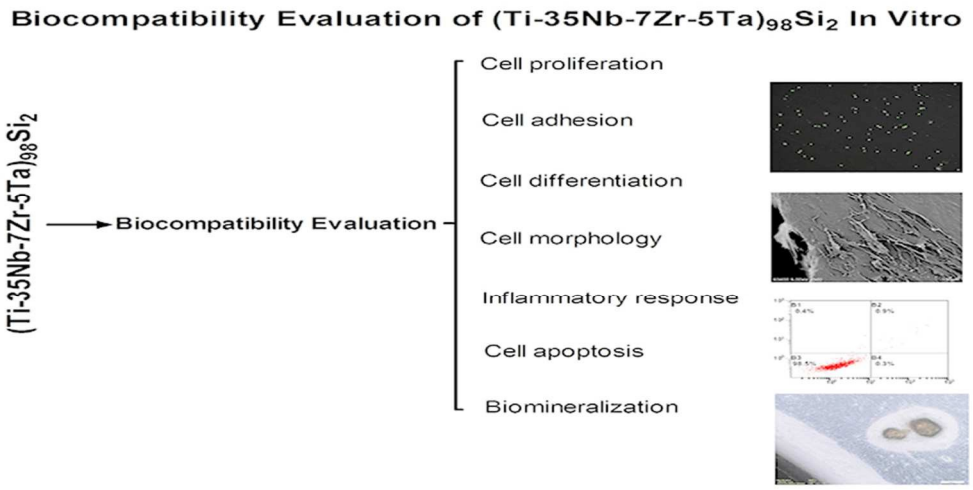

80x39mm (300 x 300 DPI)

RSC Advances Accepted Manuscript